Assessing CO_2 Absorption of Urban Trees Using NDVI, SAVI, and MSARVI in Salatiga, Indonesia

Andita, A.[1*] and Hidayati, N. I.[2]
[1]Cartography and Remote Sensing, Faculty of Geography, Universitas Gadjah Mada, Indonesia
E-mail: aningandita@mail.ugm.ac.id
[2]Department of Geographic Information Science, Faculty of Geography, Universitas Gadjah Mada, Indonesia
E-mail: iswari@ugm.ac.id
**Corresponding Author*

DOI: https://doi.org/10.52939/ijg.v221i4.4063

Abstract
Urban areas are influential in contributing to CO_2 emissions because, in urban areas, there can be an increase in land use and higher community mobility. Trees can reduce CO_2 emissions through photosynthesis, which absorbs CO_2 emissions. Nowadays, remote sensing technology can estimate the number and presence of trees and their CO_2 absorption capacity. Therefore, this study aims to find the best vegetation index approach method and assess the CO_2 absorption capacity of trees in Kalicacing and Mangunsari Urban Villages in Salatiga City using remote sensing. The method used to obtain data on the number of trees and tree species is crown delineation using orthophoto data. Meanwhile, for the estimation of CO_2 absorption, data on Diameter at Breast Height (DBH) and tree height were measured using Worldview-2 imagery with vegetation indices. The estimation model used three vegetation indices: Normalized Difference Vegetation Index (NDVI), Soil Adjusted Vegetation Index (SAVI), and Modified Soil and Atmospheric Resistant Vegetation Index (MSARVI). Statistical analysis is used to generate regression equations, and RMSE is used to determine the model's error rate. This study found that orthophoto data, Worldview-2 image data, and measurement and observation data in the field can map the ability of each tree species to estimate CO_2 absorption with a reasonable prediction model. Approximately 10,102 trees with 54 tree species are identified in Kalicacing and Mangunsari villages. NDVI, SAVI, and MSARVI have error rates of around 0.2. The MSARVI index had the smallest RMSE of 0.285. The range of ability of trees in Kalicacing and Mangunsari Urban Villages to absorb CO_2 emissions is 0.32 to 2.26 tons/tree. Trees that have the highest CO_2 absorption capacity are rudraksha trees (Elaeocarpus sphaericus) and rubber banyan trees or rubber plants (Ficus elastica).

Keywords: Carbon Dioxide Absorption, NDVI, SAVI, MSARVI, Tree

1. Introduction

The warmest year after the pre-industrial period, which saw an average temperature increase of 0.12 to 1.45 degrees Celsius from 1850-1900 climate observations, is 2023 [1]. The gases carbon dioxide (CO_2), methane (CH_4), and nitrous oxide (N_2O) continue to increase. Carbon dioxide (CO_2) is the most significant contributor to the increase in greenhouse gases at 415.7 ± 0.2 ppm in 2021 [2]. All three gases increased in concentration in 2023 [1]. Carbon dioxide emissions are caused by increased fossil fuel emissions, industrial activities, and land use changes; these activities usually occur in urban areas [3]. Urban areas significantly contribute to large amounts of carbon dioxide (CO_2) in the atmosphere, which can lead to increased greenhouse gas emissions [4]. Carbon dioxide (CO_2) emissions in urban areas will be able to increase in line with economic development in urban areas due to increased built-up land for settlements, increased household emissions, industry, and motor vehicle emissions that can cause air pollution [5].

Trees as green vegetation can reduce carbon dioxide (CO_2) emissions in urban areas [6]. This is because green plants need carbon dioxide (CO_2) to produce oxygen (O_2) during photosynthesis; therefore, the role of green vegetation in urban areas is crucial to improving air quality [7]. Green open space in urban areas is essential in urban ecology because it can convert CO_2 into O_2, maintaining the balance of gases in the air [4].

The presence of urban parks, urban forests, roadside trees, and trees around rivers can help reduce carbon dioxide (CO_2) emissions into the atmosphere due to various community activities in urban areas where the presence of trees can be a balance between ecological conditions and urban life that has many activities [8]. In green vegetation, especially trees, a component of organic content called biomass is found above the ground and below the surface [9]. Trees utilize carbon stocks in tree biomass to absorb carbon dioxide (CO_2), so the content of tree biomass in urban areas is essential to know to reduce emissions and greenhouse gases that can cause global warming [10]. The approach for calculating tree biomass in urban areas is to estimate above-ground biomass (AGB) obtained by measuring the diameter at breast height (DBH) and tree height. Tree allometric equations can be used to calculate the estimated biomass content of urban trees [4].

Nowadays, remote sensing technology can estimate the number and presence of trees and their CO_2 absorption capacity. Aerial photographs and multispectral images can be used to calculate the number of trees, tree species, and the estimated carbon dioxide (CO_2) absorption capacity of trees in urban areas. Aerial photographs have a very detailed spatial resolution because the resolution is very high up to cm [11]. The results of processing aerial photos into orthophotos can be used to delimit individual tree crowns through the crown delineation method and recognize tree species from their canopy characteristics. Meanwhile, Worldview-2 multispectral imagery can determine each tree species' estimated carbon dioxide (CO_2) absorption capacity. Worldview-2 imagery can be used to calculate the ability of carbon dioxide (CO_2) absorption because it has a high spatial resolution and a variety of bands, so it can be utilized to obtain detailed spectral values. A commonly used approach is the vegetation index transformation that utilizes specific spectral bands of the optical image. Normalized Difference Vegetation Index (NDVI), Soil Adjusted Vegetation Index (SAVI), and Modified Soil and Atmospheric Resistant Vegetation Index (MSARVI) are vegetation indices that can be used for empirical modeling of carbon dioxide (CO_2) absorption capacity.

Each index has a different accuracy and application capability [12]. This depends on the specifications of the image used and data collection during field measurements [12]. NDVI is a vegetation index that can detect the greenness of vegetation using the red band and infrared band to perform mathematical calculations to produce index values in the range of -1 to 1 [13]. SAVI is an improvement of NDVI that considers background interference in the form of soil brightness when recording vegetation with a low leaf density. SAVI utilizes the near-infrared band, the red band, and the ground brightness correction factor (L). L is a correction factor for background tree canopy [14]. The value of the L factor is 0.5. The value was set to accommodate the application of SAVI to land cover types [15]. SAVI was developed into MSARVI, which can reduce the effects of ground background and atmospheric disturbances. MSARVI is a development between SARVI (Soil and Atmospherically Resistant Vegetation Index) [16] and ARVI (Atmospherically Resistant Vegetation Index) [17] and [18], which is a development of SAVI because it is sensitive to the atmosphere so that the MSARVI formula adds a blue band. Due to different abilities, the three vegetation indices will be used to determine the accuracy and ability to model trees' carbon dioxide (CO_2) absorption in urban areas.

Salatiga City is one of the cities in Central Java Province, Indonesia, which is an expansion of Semarang Regency. The city center of Salatiga City is located in Sidomukti Subdistrict, especially in Kalicacing Urban Village, which is the center of facilities related to the government, markets, education, town square, and services. The activities cause motorized vehicle drivers to use the roads consistently to ensure mobility within the community. Furthermore, Mangunsari Urban Village is the center of Sidomukti District and has several collector roads, such as Salatiga-Kopeng. Kalicacing tends to be dominated by built-up land, specifically dense settlements, and buildings. Meanwhile, Mangunsari Urban Village is the center of urban forest green spaces such as the Ario Wirawan Lung Hospital Complex, the Center for Disease Vector and Reservoir Research and Development Complex, and Salatiga City Regional Hospital [19]. However, in both urban villages, some tree species are also found in the city center square and on the roadside as public green open spaces, and there are also trees in home yards, office yards, or service yards so that they become private green open spaces. This research is essential because integrating remote sensing data with measurement and observation activities related to biodiversity and estimation of carbon dioxide (CO_2) absorption capacity can reduce the increase of greenhouse gases and global warming [20]. It is hoped that the results of this research can be one of the solutions in urban areas to select suitable tree species to reduce carbon dioxide emissions and as one of the technological implementations in tackling climate change as point number thirteen in the SDGs Environmental Development pillar.

Therefore, the objectives of this study are to determine the error in the utilization of vegetation index to estimate carbon dioxide (CO_2) absorption capacity and to estimate the carbon dioxide (CO_2) absorption capacity of each tree species in Kalicacing and Mangunsari Urban Villages, Salatiga City from the vegetation index model.

2. Methods

2.1 Research Area

Salatiga City is in Central Java Province, directly neighboring Semarang Regency (Figure 1). The elevation of Salatiga City is 602-680 meters above sea level [19]. More specifically, the research site is located in Kalicacing and Mangunsari urban villages, the city center of Salatiga City. Both villages are situated in Sidomukti subdistrict, which has an area of 10.8 km^2. The location of Mangunsari Urban Village is 2.76 km^2, and the area of Kalicacing Urban Village is 0.72 km^2. Despite the relatively small size of these two Urban Village, they are centers of government such as the Salatiga Mayor's Office, the Salatiga City Regional House of Representatives Office, and the Salatiga Police Station; centers of education such as schools and universities; industries; and as residential centers, they generate a lot of mobility. Since these two urban villages are the urban center and sub-center of Salatiga City, the mobility and activity of the people are relatively high. However, there is still standing vegetation in the form of trees that serve as green open spaces, so it is essential to identify the types/species of trees in the two urban villages and their ability to absorb carbon dioxide (CO_2).

2.2 Data Collection

Two remote sensing data were used to determine the carbon dioxide (CO_2) absorption capacity of trees in Kalicacing and Mangunsari urban villages, and there are orthophoto data of Salatiga City for the 2023 recording year and Worldview-2 imagery recorded on October 11, 2023 (Table 1). The orthophoto data was used to generate information on the number of trees and the canopy extent of each tree. At the same time, the CO_2 sequestration capacity was estimated from empirical modeling using Worldview-2 imagery. The Worldview-2 image used has a temporal resolution of 1 day, a spatial resolution of 1.8 meters for multispectral type, a radiometric resolution of 11 bits, and eight multispectral bands consisting of coastal blue, blue, green, yellow, red, and red edge, NIR1, and NIR2 bands. Worldview-2 imagery generates vegetation indices in NDVI [21], SAVI [22] and [23], and MSARVI.

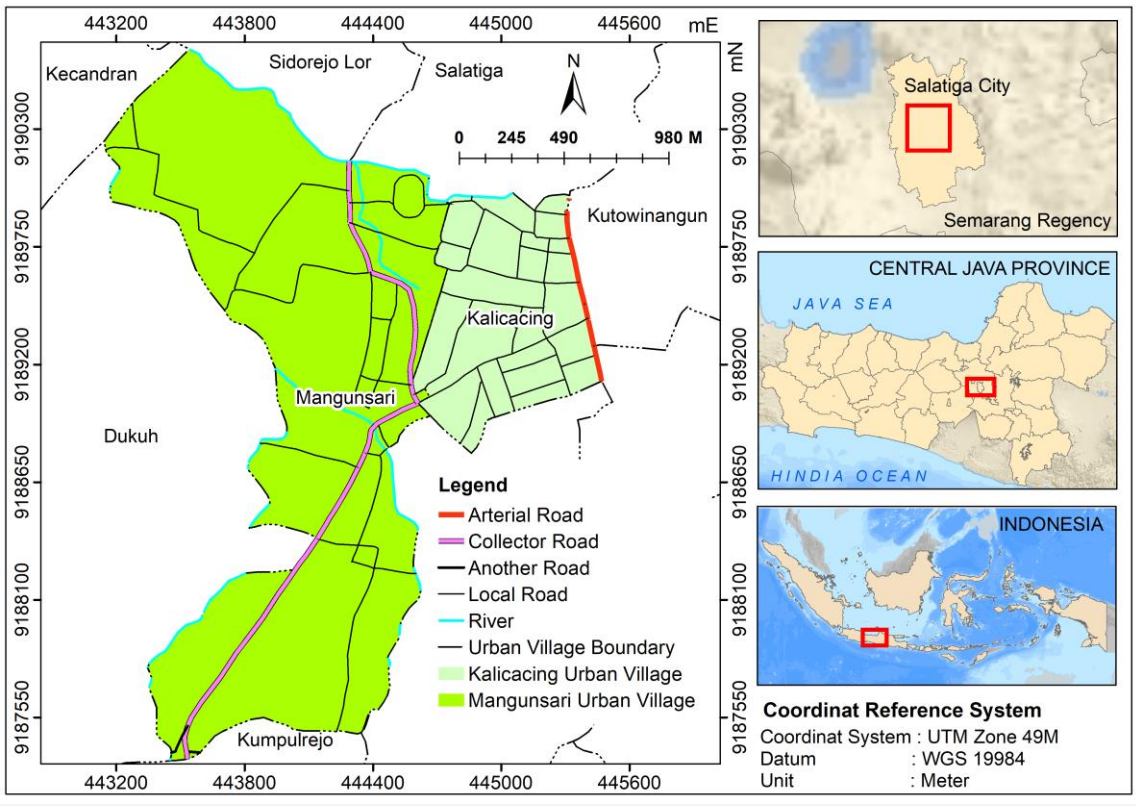

Figure 1: Salatiga, Indonesia administration map (Source: Map of administration boundary from Geospatial Information Agency)

The three vegetation indices will be used as models for carbon dioxide (CO_2) absorption estimation resulting from the regression equation of image pixel values as a prediction model with biomass values obtained from DBH and tree height measurements in the field as actual data. DBH was obtained by measuring the trunk's circumference, while tree height was obtained using a distometer and laser rangefinder. To obtain data related to tree species, the researchers conducted three stages of identification: interpretation of elements from tree crowns using Google Street View and observation and inventory during field activities. The element of interpretation of tree characteristics can be recognized with optical imagery, such as aerial photography because it can see the shape, size, and morphology of the crown [24]. Google Street View was used to add tree species identity to polygons where the attribute table was empty. This is because not all trees can be recognized quickly through the elements of crown interpretation [25]. Google Street View is used to see the morphology and detect trees near the road. Observations with Google Street View were conducted before field activities; thus, only polygons that had not identified tree species during the pre-field stage were completed during field activities. Observations were made by observing trees located in places on Google Street View, such as gardens behind houses or in shrubs that cannot be reached. However, tree species were restricted according to the identification results through interpretation elements and Google Street View. Trees observed through Google Street View show trees near the road, essential for absorbing carbon dioxide. For the sampling of DBH and tree height measurements, the number of samples was determined by the proportion of the number of tree polygons. The calculation of the number of samples was carried out using the binomial probability method [25]. The equation used to calculate binomial probability is shown in Equation 1.

$$N = \frac{Z^2 pq}{E^2}$$

Equation 1

Where:

- N = The number of samples
- Z = 2 (normal standard deviation for 95% confidence)
- p = Expected accuracy (85%)
- q = 100-p
- E = Allowable error (5%)

A stratified random sampling method was used based on tree species. Sampling is based on tree species strata found in the pre-field stage using elemental interpretation methods and remote activities that utilize Google Street View. Random sampling was used because tree species represent strata for sampling based on species and because they can represent different biophysical capabilities [26]. Meanwhile, DBH and tree height measurements were measured in a plot to minimize shifting points on the GPS. The plot size based on these pixels is used to reduce the shift of pixels around 0.5-1 pixels when collecting data in the field that uses GPS equipment to obtain coordinate points. The plot size is defined in Equation 2 [25]. Therefore, the plot size in this study was 4 by 4.

$$A = P(1 + 2L)$$

Equation 2

Where:

- A = Dimensions of sample plot sizes in the field (m)
- P = Spatial resolution or pixel size of the image (m)
- L = Minimum error accuracy (0.5)

The data used in this research are presented in the following table with the sources.

Table 1: Data used

Data	Data Acquisition Source
Ortophoto of Salatiga City 2023	Public Works and Spatial Planning Office of Salatiga
Worldview-2 multispectral imagery 2023	Purchased through vendor Digital Globe
DBH (Diameter at Breast Height) of each identified tree species	Field measurement
Height of identified tree species	Field measurement
Tree species	Interpretation crown tree, Google Street View, and field observation
Administrative boundary of Village, road, and river shapefile	InaGeoportal (https://tanahair.indonesia.go.id/portal-web/)
Wood density	Literature review
Characteristics of tree species	Literature review

2.3 Data Processing

2.3.1 Radiometric correction Worldview-2

The radiometric correction stage is a pre-processing stage that aims to improve the accuracy value of image pixels related to spectral reflectance as a basis for enhancing images [14]. There is an atmospheric correction in the radiometric correction stage. The atmospheric correction stage is a stage to eliminate the effects of scattering, reflection, and absorption of various components in the atmosphere [17]. Radiometric correction of Worldview-2 imagery uses Top-of-atmosphere radiometric correction provided by ENVI software with the following formula.

2.3.2 Vegetation index processing

Vegetation index is used as an independent variable [27]. The NDVI, SAVI, and MSARVI vegetation indexes used to model the estimated carbon dioxide (CO_2) absorption capacity have different formulas. The formula for NDVI is shown in equation 4 [27]:

$$NDVI = \frac{\rho NIR2 - \rho RED}{\rho NIR2 + \rho RED}$$

Equation 4

Where:

NDVI = Normalized Difference Vegetation Index
$\rho NIR2$ = Spectral reflection acquired from Near Infrared-2 Band
ρRED = Spectral reflection acquired from Red Band

In equation 4, *NIR2* and the *RED* band produced the best accuracy and high precision for urban vegetation mapping at 96.29% [27]. SAVI is defined in equation 5 [17]:

$$SAVI = (1+L)\left(\frac{\rho NIR1 - \rho RED}{\rho NIR1 + \rho RED + L}\right)$$

Equation 5

Where:

SAVI = Soil Adjusted Vegetation Index
$\rho NIR1$ = Spectral reflection acquired from Near Infrared-1 Band
ρRED = Spectral reflection acquired from Red Band
L = 0.5

In equation 5, *NIR1* is used for the *SAVI* vegetation index when using Worldview-2 imagery [22]. Equation 6 is used to determine MSARVI index [12].

$$MSARVI = \frac{2\rho NIR1 + 1 - \sqrt{(2\rho NIR1 + 1)^2 - y(\rho NIR1 + \rho RB)}}{2}$$

Equation 6

Where:

MSARVI= Modified Soil and Atmospheric Resistant Vegetation Index
$\rho NIR1$= Spectral reflection acquired from Near Infrared-1 Band
$\rho RB = \rho RED$ – y($\rho BLUE - \rho RED$)
ρRED = Spectral reflection acquired from Red Band
$\rho BLUE$ = Spectral reflection acquired from Blue Band
y = 1

The *MSARVI* value must be normalized to be close to the minimum and maximum values of vegetation in the image [16]. Therefore, equation 7 presents the normalized *MSARVI*.

$$MSARVI_{norm} = \frac{MSARVI - MSARVI_{min}}{MSARVI_{max} - MSARVI_{min}}$$

Equation 7

Where:

$MSARVI_{norm}$ = Normalized Modified Soil and Atmospheric Resistant Vegetation Index
$MSARVI_{min}$ = Minimum *MSARVI*
$MSARVI_{max}$ = Maximum *MSARVI*

2.3.3 Biomass calculation

The results of the circumference and diameter measured were further used to calculate the volume and biomass of the tree using equation 8 [29]:

$$V = 0.25\pi HF(DBH)^2$$

Equation 8

Where:

V = Tree volume (m^3)
H = *Tree h*eight (m)
F = Correction coefficient (0.6)
DBH = Diameter at Breast Height (m)

The *F* value (0.6) is a correction factor obtained from the ratio of the actual rod volume to the cylinder volume at the same diameter and height [28]. The calculation was important due to the need for tree volume to determine biomass. This can be observed from equation 9:

$$B = \frac{\sum(\rho V)BEF_T}{1,000}$$

Equation 9

Where:
B = Biomass (ton)
P = Wood density (tree species) (kg/m^3)
V = Tree volume (m^3)
BEF_T = Biomass expansion factor

Biomass Expansion Factors (*BEF*) are factors used to multiply stem biomass by the above-ground biomass when measuring biomass estimates for above-ground biomass. *BEF* of the stand depended on each tree species, but 1.74 was used when the value was not found [28]. If the density value of the tree species is unknown, the allometric used is from [29], which was also used by [10] for urban biomass. The allometric equation presents in equation 10 [30].

$$B = \frac{42.69 - 12.8(DBH) + 1.242(DBH)^2}{1,000}$$

Equation 10

Equation 10 is adjusted based on the annual rainfall or climate zone according to [9]. The following is the allometric equation from [30] and the rainfall range (mm/year). Salatiga City has an average rainfall of 2,425 mm/year [19]. Therefore, the allometric equation used when no reference tree density was found for a particular tree species/type would be the allometric equation for humid rainfall (1,500-4,000 mm/year).

2.3.4 Statistic analysis

The existing samples were divided into two groups, including model and validation. The model samples were used for statistical analysis and empirical modeling, while the validation samples were used to determine the RMSE. The statistical analysis conducted included normality, correlation tests, and regression using the field data as the dependent variables, while NDVI, SAVI, and MSARVI values were independent variables. The regression analysis results were used to produce the equation $Y = ax + b$, which was later applied to empirical modeling of biomass using Worldview-2 multispectral image (Table 2). The modeling results were subjected to an accuracy test using equation 11:

$$RMSE = \sqrt{\frac{\sum (A_t - F_t)^2}{n}}$$

Equation 11

Where:
$RMSE$ = Root Mean Square Error
A_t= Biomass results from measured in the field (actual value)
F_t= Value generated from empirical biomass model (model value)
n = Validation sample data amount

The determination of the empirical biomass model was followed by the calculation of carbon stock using the equation 12 [12].

$$C_b = BF$$

Equation 12

Where:
C_b = stored carbon stock content (ton)
F = percentage value of carbon content (0.47)

The F value is a constant value that shows the percentage of carbon content in biomass based on SNI 7724-2011. The 0.47 or 47% value is obtained from laboratory calculations and measurements. Carbon stock was converted to estimate CO_2 absorption capacity [31]. This was achieved using the equation 13.

$$CO_2ab = 3.67C_b$$

Equation 13

Where:
CO_2ab = CO_2 absorption capacity

The modeling results were extracted based on polygon species using zonal statistics. This was achieved based on the average pixel value of the identified polygon. The methodology of this study is presented in Figure 2.

Table 2: Allometric equation

Tropical Climate Zone and Rainfall (mm/year)	Allometric Equation	Diameter Range (cm)
Dry (<1,500)	$B = exp\{-1.996+2.32*ln(DBH)\}$	5-40
Humid (1,500-4,000)	$B = 42.69-12.800(DBH)+1.242(DBH^2)$	5-148
Wet (>4,000)	$B = 21.297-6.953(DBH)+0.740(DBH^2)$	4-112

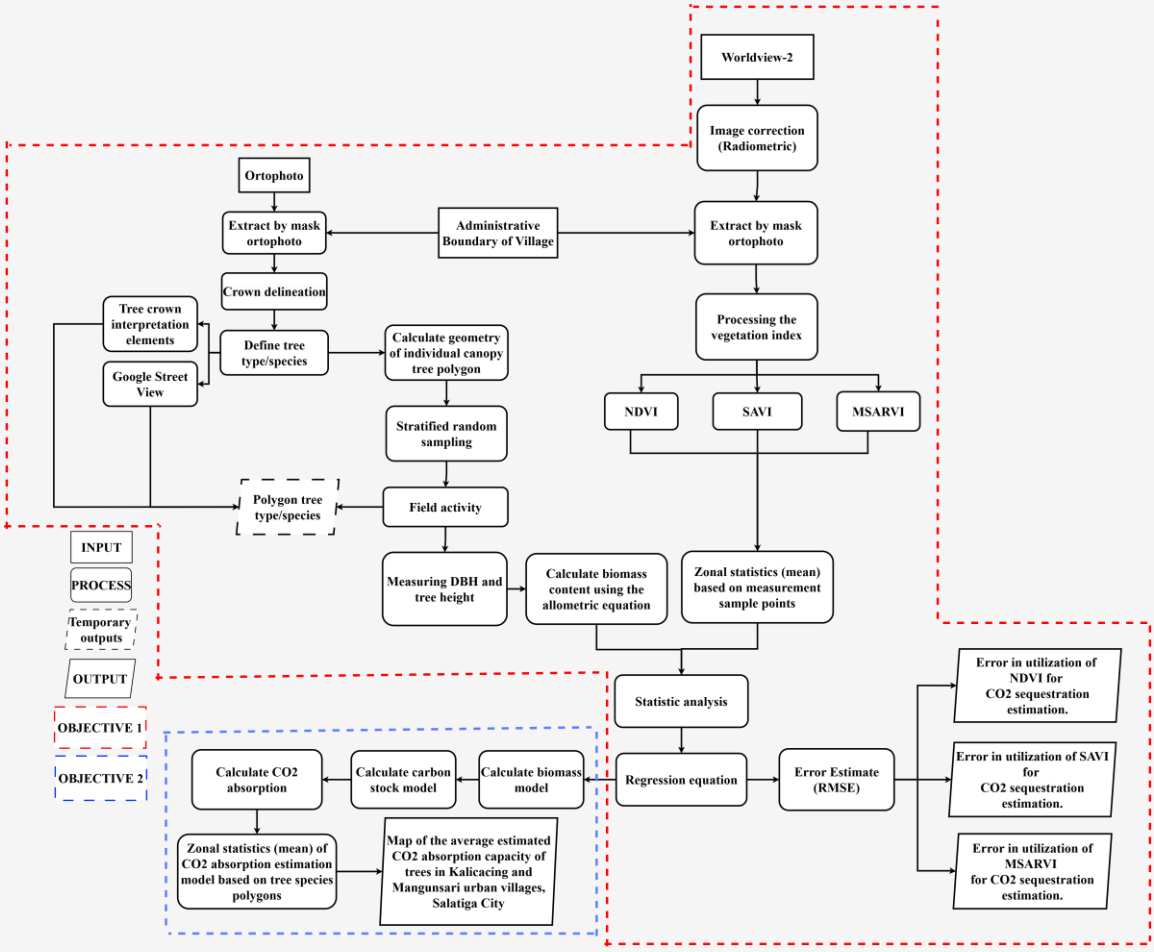

Figure 2: Carbon absorption capacity determination

3. Result and Discussion

3.1 Type/Species of Trees in Kalicacing and Mangunsari Urban Village

A total of 10,102 polygons show the number of trees identified in Kalicacing and Mangunsari Urban Village. Approximately 54 types or species of trees have been found in Kalicacing and Mangunsari Urban Village. The number of trees in Kalicacing Urban Village is less than in Mangunsari Urban Village. The number of trees in Kalicacing Urban Village is approximately 1,603, while the number of trees in Mangunsari Village is approximately 8,499. Kalicacing Urban Villages has fewer trees because it has a lot of built-up land in dense settlements, government buildings, and public or service facility buildings. From the tree species polygon, the canopy cover area of trees in the two villages was only 13.68% of the total area of the two villages, so the remaining 86.32% of the dominant land use of the two urban villages was settlements, buildings, public facilities, roads, agricultural land, and open land so that the existing canopy area in the two villages tended to be still small. The percentage of canopy cover area in Kalicacing Urban Village compared to the total area of Kalicacing Urban Village is only 9.37%, which is 0.72 km2, so the remaining 90.63% tends to be built-up land, such as settlements, buildings, roads, and open land such as fields or yards of houses and offices. Meanwhile, the canopy cover area in Mangunsari Urban Villages is 40.26%, so the remaining 59.74% is dominated by residential land use, built-up land, and rice fields.

3.2 Vegetation Index

3.2.1 Normalized Difference Vegetation Index (NDVI)

Kalicacing and Mangunsari Urban Villages show NDVI values that range from 0.51 to 0.99. The NDVI values were then classified into five using the Natural Breaks method provided by ArcGIS (Figure 3). This method was chosen because it is more representative than other classification methods with the same number of classes.

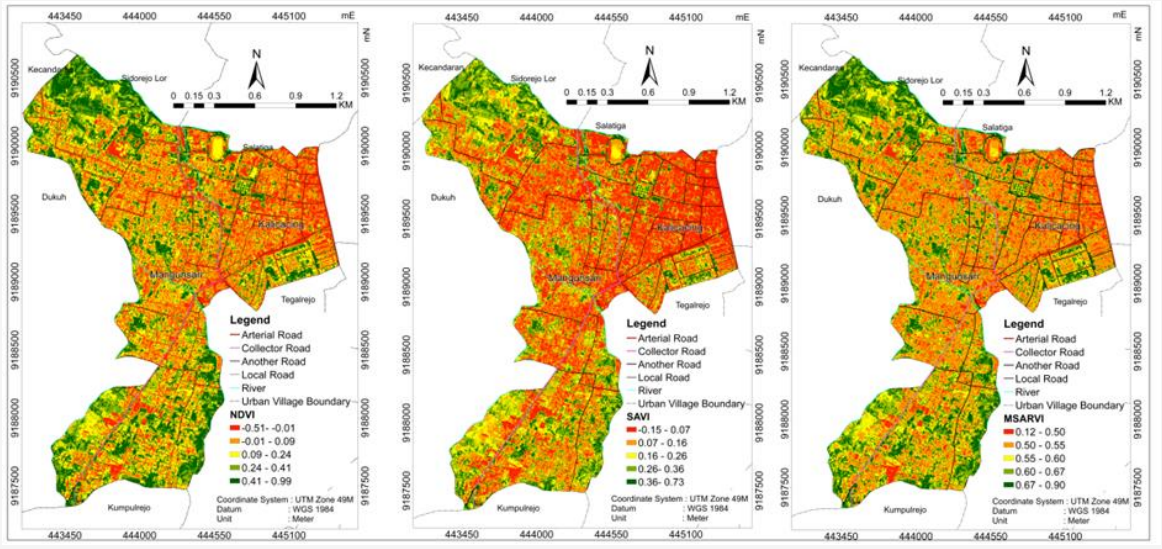

(a) (b) (c)

Figure 3: Vegetation index (a) NDVI, (b) SAVI, and (c) MSARVI

The higher the index value, the denser the leaves and crowns of the vegetation object and the higher the greenness of the pixel. Green vegetation values are shown in the range of 0.24-0.99. Non-vegetation object values are shown in red to orange, with a value range of -0.51 to 0.09. Values that are negative and close to zero indicate non-vegetation objects. Meanwhile, NDVI values in the range 0.09-0.24 indicate vegetation objects such as grass. These NDVI values show that the resulting NDVI range is already from -1 to 1. NDVI will produce an index value in the range of -1 to 1. The closer to 1 indicates that the object is a vegetation object, while the closer to -1 suggests that the object is not a vegetation object [15].

3.2.2 Soil Adjusted Vegetation Index (SAVI)

SAVI values in Kalicacing and Mangunsari Urban Villages range from -0.15 to 0.73 (Figure 3). SAVI results are more assertive towards non-vegetated lands, such as building roofs, roads, and land, shown in red and orange colors with values of -0.15 to 0.16. Similar to NDVI, SAVI shows that non-vegetation objects have lower values than vegetation objects. In Kalicacing Urban Village, which is dominated by building objects, it is more evident that these objects are not vegetation objects whose value ranges are dominant in the -0.15 to 0.07 range. This is because SAVI has been set to reduce the background of the tree canopy so that soil objects recorded in the tree canopy will be clarified as soil objects [14]. Meanwhile, vegetation objects in SAVI results are not very prominent in showing the level of greenness compared to NDVI. Vegetation objects, especially trees, are visible in the range of 0.26 to 0.73. For the distribution of vegetation objects with a high level of greenness (0.36-0.73), the SAVI results have the same pattern as the NDVI results. Trees are more clustered on the north side and southeast side. The north and northwest sides are rice fields close to mixed gardens, while the southeast side is a community forest with mixed gardens with tall trees, and the canopy is still dense.

3.2.3 Modified Soil and Atmospheric Resistant Vegetation Index (MSARVI)

Visually, MSARVI looks more similar to NDVI. The range of MSARVI values in Kalicacing and Mangunsari Urban Village ranges from 0.12 to 0.90 (Figure 3). The MSARVI value differs from the NDVI and SAVI values, which have a minimum minus value. Non-vegetation objects in MSARVI results tend to be in the range of 0.50 to 0.55, which is orange. In SAVI and NDVI, this value is included in the category of vegetation objects, while the MSARVI results for vegetation objects are in the range of 0.67 to 0.9. MSARVI values for vegetation objects tend to be very high. This is because MSARVI is a modification of SAVI and ARVI that corrects for soil and atmospheric disturbances so that vegetation objects with dense canopies and high levels of greenery will have actual values close to actual conditions [14]. Regarding distribution, MSARVI values for vegetation objects are similar to NDVI and SAVI. Vegetation objects are more abundant in the north, northwest, south, and southeast sides.

3.3 Actual Biomass

The number of trees measured was 275. This number differs from the sample points calculated using Equation 1. One plot can contain one to four trees because the sample trees measured are close to other trees, so the measured trees can be more than the number of sample points showing the tree species canopy polygon. When two or three trees are measured in a plot for a single sample point, the additional trees tend to be lower in height than the crown size of the trees used as samples. In addition, the measured trees also have many branches, so in one tree canopy, several branches can be measured when the free branch height is less than 1.3 meters or only one stem when the free branch height is more than 1.3 meters from the ground [32].

From the calculation results using allometric equations in equations 9 and 10, the types/species of trees that have high biomass include the Japanese fern tree (*Filicium decipiens*), stink bean tree (*Parkia speciosa*), and African tulip tree (*Spathodea campanulata*) which reach 0.9673 kg. These trees are trees that have relatively large diameters and tree heights. The biomass produced tends to be influenced by the volume. These trees are generally found in Pancasila Square and around the highway. Meanwhile, the types/species of trees that have low biomass content include the golden trumpet tree (*Handroanthus chrysotrichus*), devil's tree (*Alstonia scholaris*), and red lip tree (*Syzygium myrtifolium*), which have a biomass content of only 0.0154 tons to 0.0829 tons. These trees are usually found in cemeteries, house yards, and on the sides of roads. The low height of the trees indicates that they are relatively young. And so is the opposite. The same is also valid for diameter. If the diameter is more expansive, the tree's age will be older, and so will the opposite. According to [33], most vegetation has a linear relationship between height, diameter, and plant growth rate, which also increases in height and diameter over time. The height growth will affect and be in line with the development of branches on the trunk so that the tree crown will also increase [33]. Therefore, height and diameter affect tree volume, crown, and biomass. However, the average measured biomass of the tree samples was 0.4 to 0.7 tons for one tree.

3.4 Statistical Analysis

From the 204 measurement sample points, not all data is divided into model and validation samples. This is because the sample data tends not to be normally distributed when tested for normality. Therefore, from 204 tree sample points, geometry was calculated for the tree polygon to determine the area of tree canopy cover that had been measured DBH and tree height. The canopy cover area was then classified into four classes. The classification of canopy cover area is shown in Table 3. The tree canopy cover classes were obtained using the quartile method from the tree polygons measured in the field. The quartile method was chosen to facilitate the division of canopy size levels. These classifications were used as strata and the basis for the actual biomass sampling for modeling. The assumption was that biomass content is correlated with canopy size. The extent of tree canopy cover, especially within an individual tree was conducted by [34], from lidar data representing Above Ground Biomass (AGB), which showed that the extent of tree canopy cover can represent tree characteristics and is relevant to tree volume and biomass. After the data is proportional and the actual content of tree biomass represents each canopy area class, statistical analysis can be conducted to test the field sample data that will be used for modeling. The field sample data used for modeling totaled 55 sample points. These points are enough for modeling because in the study of [10], the ideal number of sample points for taking tree stem measurement data with a large population is 30 to 200, and each class must be represented. The sample points containing the coordinate locations were exported to shapefile to make a 4x4 square buffer that matches the plot size. The buffer was then used to conduct zonal statistics for biomass from the vegetation index with the pixel values of the NDVI, SAVI, and MSARVI indexes because the higher the biomass level is, the higher the greenery level [12]. Thirty-two samples were used for the model sample, while the other 23 sample points were used to calculate the error with RMSE. The model samples are used for normality tests, correlation tests, and linear regression analyses to obtain the equation $Y = aX + b$ with R^2 value indicating the coefficient of determination. The normality test uses SPSS with the Kolmogorov-Smirnov method for a significance value 0.05 [10].

Table 3: Classification and range of tree canopy cover area [35]

Tree canopy area classification	Range tree canopy area (m^2)
Small size canopy	<23.53
Medium size canopy	23.53-49.85
Wide size canopy	49.85-94.24
Vast size canopy	>94.242

The following are the results of the normality test of the actual biomass, NDVI, SAVI, and MSARVI data variables. From the normality test results in Table 4, all variable data are typically distributed with more than 0.05 [10]. Normally distributed data were then tested for correlation to determine the strength and direction of the correlation between actual biomass data and vegetation index values. The correlation test uses the Pearson method with SPSS. Table 5 shows the results of the correlation test. The correlation results have almost the same value, which is 0.6. The correlation value shows a moderate correlation between actual biomass and NDVI, actual biomass and SAVI, and actual biomass and MSARVI. This is because the correlation value of 0.6 is in the range of 0.41-0.7, which shows a moderate correlation [36]. The direction of the correlation is positive, which means that the higher the tree biomass content, the higher the NDVI, SAVI, and MSARVI index pixel values. And the same goes for the other way around. The highest correlation is between actual biomass content and NDVI, while the lowest is between actual biomass and SAVI.

Regression analysis is performed when the data is tested regularly, and correlation is tested. Linear regression will result in the equation $Y = aX + b$. With Y being the criterion or empirical model of biomass produced, X being the predictor, which in this case is the GPP index indicating biomass, A being the predictor coefficient, and b being the intercept. The coefficient of determination (R^2) indicates the level of relationship and the ability of the independent variable (X) to explain the dependent variable (Y) [37]. The greater the R^2 value, the higher the correlation and the more influential the independent variable is to explain the dependent variable by the conditions in the field. The independent variables (X) are NDVI, SAVI, and MSARVI, while the dependent variable (Y) is actual biomass. The R^2 results and regression equation are presented in Table 6.

The R^2 result of NDVI with actual biomass has a higher R^2 value than SAVI and MSARVI. 47.1% of NDVI can explain the actual biomass for modeling biomass estimation to carbon dioxide (CO_2) absorption estimation, while other factors influence 43.9%. Other factors that are not modeled can be influenced by image factors such as spectral resolution, spatial resolution, radiometric resolution, and temporal resolution. In addition, measured tree morphology, such as DBH, cannot be modeled in the index value because the vegetation index value shows the vegetation canopy's greenness based on the satellite sensor's brightness value [38]. This is also true in SAVI and MSARVI. In addition, land use, especially built-up land in urban areas, will affect pixel values, causing mixed pixels with vegetation object values.

3.5 Error Rate of the Model Biomass Estimation

The error rate of the biomass estimation model obtained from the regression equation was then calculated with the RMSE calculation. The RMSE calculation for each model is shown in Table 7.

Table 4: Normality test

	Kolmogorov-Smirnova		
	Statistic	**df**	**Sig.**
Biomass actual	0.124	32	0.200*
NDVI	0.105	32	0.200*
MSARVI	0.121	32	0.200*
SAVI	0.097	32	0.200*

* is the lower bound of the true significance

Table 5: Correlation test

Indices	**NDVI**	**SAVI**	**MSARVI**
Actual biomass	0.686**	0.652**	0.663**

**Correlation is significant at the 0.01 level (2-tailed)

Table 6: Regression equation wit hactual biomass and R^2 value

Indices	**R^2**	**Regression equation**
NDVI	0.471	y = 1.0781x + 0.1175
SAVI	0.440	y = 1.5458x + 0.0628
MSARVI	0.442	y = 2.8290x - 1.3369

Table 7: RMSE for biomass model estimation

Vegetation index model for biomass estimation	RMSE
NDVI	0.290
SAVI	0.287
MSARVI	0.285

Table 8: Range RMSE and quality of performance

Range of RMSE	Performance
< 0.009	Excellent prediction accuracy
0.009 < RMSE < 0.09	Good prediction accuracy
0.09 < RMSE 0.5	Reasonable prediction
> 0.5	Inaccurate prediction

Table 9: Classification and range of CO_2 absorption estimation

Classification of CO_2 absorption	CO_2 absorption range (ton/tree)
Low	<0,32
Moderate	0,32-0,86
High	0,86-2,26

The RMSE results for models with NDVI, SAVI, and MSARVI methods are included in the category of reasonable prediction. This refers to [39] regarding the RMSE range for the performance model, which can be seen in Table 8. Of the three vegetation index methods, MSARVI has a lower error than NDVI and SAVI. This shows that the biomass model for estimating CO_2 uptake using MSARVI has a lower error rate than the NDVI and SAVI models because the value is smaller. MSARVI has a lower error rate than the NDVI and SAVI models because MSARVI is an improvisation of the NDVI and SAVI indices that can reduce soil disturbances and reduce atmospheric disturbances such as removing Rayleigh and ozone components even though the image has been corrected [14]. In addition, it is also affected by the MSARVI pixel value and the regression equation used.

3.6 Mapping and Estimation of CO_2 Absorption

The estimated CO_2 absorption is calculated from the biomass estimation model obtained from the regression equation. The biomass estimation model is then converted into carbon stock to the CO_2 absorption capacity of the tree. The carbon dioxide (CO_2) absorption capacity with the biomass approach was carried out by applying the results of the carbon stock model with the ratio of the relative mass of carbon dioxide (CO_2) and the relative atom of carbon (C) (Table 9). The relative mass of carbon dioxide (CO_2) is 44, while the relative atom of carbon (C) is valued at 12. Hence, the ratio is 3.67, which indicates the level of carbon stock's ability to absorb carbon dioxide in an individual tree [4]. The modeling results were then obtained with zonal statistics to get the average pixels in one polygon unit of tree type/species.

The extraction results were then classified from the calculation of the CO_2 absorption capacity of tree samples that had been measured during field activities. This is done to help provide an overview of the ability of each type/species of tree to absorb carbon dioxide emissions according to its actual conditions. The following is a classification table and estimated CO_2 absorption range used.

The estimated CO_2 absorption capacity will be expressed for estimation in tons/tree. This is because it follows the reflectance vegetation at pixel value Worldview-2 imagery. The spectral values of vegetation may change in different recording periods [40]. In addition, the estimated daily unit of CO_2 absorption of trees can be different every day because of the solar radiation energy factor, which plays a role in the photosynthesis process and atmospheric effects during image recording [40]. However, this is a limitation of utilizing remote sensing imagery because the CO_2 absorption capacity of trees depends on the growth rate of trees to store biomass and carbon stocks.

The three maps show that most of the trees in Kalicacing and Mangunsari Urban Villages have medium and high CO_2 absorption capabilities (Figure 4). Trees with low CO_2 absorption capacity have a relatively small canopy area, while trees with a relatively large canopy have medium to high absorption capacity. The distribution of trees with low CO_2 absorption capacity is trees with a young age, which can be seen from the relatively small size of the canopy. Meanwhile, trees with high CO_2 absorption tend to have a broad and large canopy because they are relatively large and tall, which causes them to have high biomass content and CO_2 absorption.

At first glance, there is no significant difference between the NDVI, SAVI, and MSARVI models. However, there are some changes in the CO_2 absorption capacity of certain trees. The difference and change in values are due to the different index formulas and regression equations. However, using the MSARVI index for estimating CO_2 absorption has a lower error rate than NDVI and SAVI. Due to the map's limitations in presenting information related to tree type/species labels, the following is Table 10 which shows the average ability of tree types/species in Kalicacing and Mangunsari Urban Villages. The estimated value of CO_2 absorption capacity in each tree type/species depends on the value of the tree reflection recorded in the image pixels, the regression equation used, and the morphology of the tree according to conditions in the field such as DBH size, height, canopy width, and leaf color.

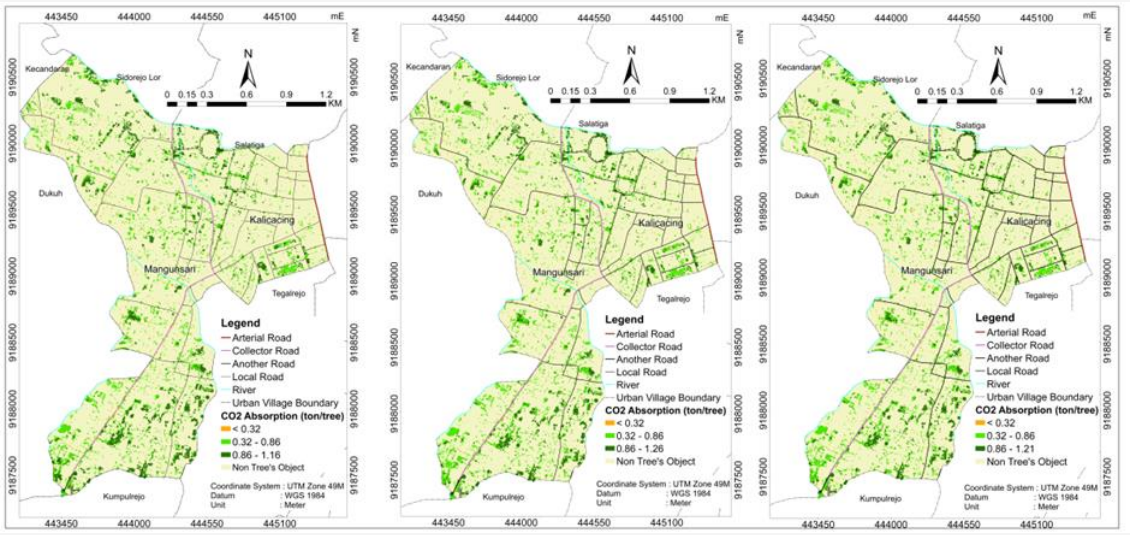

(a) (b) (c)

Figure 4: CO_2 absorption estimation of the tree for each vegetation index: (a) NDVI, (b) SAVI, and (c) MSARVI

Table 10: Ability to estimate average CO_2 absorption of tree types/species

Tree type/species	Estimate average CO_2 absorption (ton/tree)		
	MSARVI	NDVI	SAVI
Black Wattle (*Acacia mangium*)	0.777	0.804	0.774
Avocado (*Persea americana*)	0.746	0.762	0.752
Rosewood (*Pterocarpus indicus*)	0.722	0.721	0.722
Tamarind (*Tamarindus indica*)	0.614	0.639	0.621
Starfruit (*Averrhoa carambola*)	0.553	0.552	0.568
Cucumber Tree (*Averrhoa bilimbi*)	0.628	0.652	0.642
Benjamin Fig (*Ficus benjamina*)	0.817	0.836	0.810
Queen's Crape Myrtle (*Lagerstroemia speciosa*)	0.850	0.851	0.869
Chinese Arborvitae (*Platycladus orientalis*)	0.520	0.518	0.513
Damar (*Agathis dammara*)	0.795	0.809	0.778
Purple Orchid Tree (*Bauhinia purpurea*)	0.592	0.587	0.580
Langsat (*Lansium domesticum*)	0.697	0.721	0.700
Durian (*Durio zibethinus*)	0.714	0.746	0.720
Flame Tree (*Delonix regia*)	0.757	0.777	0.756
False Ashoka (*Polyalthia longifolia*)	0.560	0.564	0.572
Water Apple (*Syzygium aqueum*)	0.567	0.578	0.579

Table 10: Ability to estimate average CO_2 absorption of tree types/species (Cont.)

Tree type/species	Estimate average CO_2 absorption (ton/tree)		
	MSARVI	NDVI	SAVI
Guava (*Psidium guajava*)	0.453	0.438	0.468
Teak (*Tectona grandis*)	0.743	0.774	0.746
Rudraksha (*Elaeocarpus sphaericus*)	0.928	0.946	0.933
Pomelo (*Citrus maxima*)	0.545	0.550	0.560
Frangipani (*Plumeria alba*)	0.664	0.660	0.693
Rubber Plant (*Ficus elastica*)	0.930	0.917	0.949
Paperbark Tree (*Melaleuca leucadendra*)	0.567	0.538	0.553
Santol (*Sandoricum koetjape*)	0.751	0.781	0.756
Coconut Palm (*Cocos nucifera*)	0.748	0.775	0.753
Longan (*Dimocarpus longan*)	0.722	0.738	0.734
Japanese Fern Tree (*Filicium decipiens*)	0.872	0.871	0.893
Jamaica Cherry (*Muntingia calabura*)	0.649	0.652	0.652
Fiddle-leaf Fig (*Ficus lyrata*)	0.873	0.857	0.897
Madagascar Almond (*Terminalia mantaly*)	0.704	0.698	0.711
Birdlime Tree (*Pisonia grandis*)	0.346	0.375	0.426
Mahogany (*Swietenia mahagoni*)	0.856	0.882	0.855
Mango (*Mangifera indica*)	0.582	0.586	0.592
Mangosteen (*Garcinia Mangostana Linn*)	0.704	0.738	0.701
Island Lychee (*Pometia pinnata*)	0.788	0.808	0.795
Jackfruit (*Artocarpus heterophyllus*)	0.737	0.755	0.745
Pygmy Date Palm (*Phoenix roebelenii*)	0.626	0.631	0.651
Christmas Palm (*Veitchia merillii*)	0.558	0.568	0.557
Royal Palm (*Roystonea regia*)	0.660	0.660	0.643
Round-leaf Fountain Palm (*Livistona rotundifolia*)	0.545	0.538	0.552
Stink Bean (*Parkia speciosa*)	0.790	0.812	0.797
Merkus Pine (*Pinus merkusii*)	0.676	0.706	0.659
Red Lip Tree (*Syzygium myrtifolium*)	0.552	0.558	0.556
Devil's Tree (*Alstonia scholaris*)	0.542	0.491	0.536
Rambutan (*Nephelium lappaceum*)	0.617	0.637	0.622
Silk Tree (*Albizia chinensis*)	0.829	0.858	0.834
Soursop (*Annona muricata*)	0.552	0.559	0.560
Corn Plant (*Dracaena fragrans*)	0.561	0.567	0.556
Breadfruit (*Artocarpus altilis*)	0.613	0.622	0.641
Golden Trumpet Tree (*Handroanthus chrysotrichus*)	0.460	0.458	0.478
White Trumpet Tree (*Tabebuia riparia*)	0.749	0.748	0.765
Rain Tree (*Samanea saman*)	0.916	0.920	0.931
African Tulip (*Spathodea campanulata*)	0.761	0.764	0.766
Other Tree Species	0.762	0.787	0.769

The most influential is the spectral value of the tree canopy on the image used [41]. Therefore, the model in this study is an estimate that can illustrate the ability to absorb CO_2 trees in Kalicacing and Mangunsari Villages in Salatiga City. The type/species of tree that has the lowest CO_2 absorption capacity is the birdlime tree (*Pisonia grandis*). The birdlime tree (Pisonia grandis) is a tree that has light yellowish-green leaves, so the greenness level is low, which causes the vegetation index value in the image to be low. Meanwhile, the rudraksha tree (*Elaeocarpus sphaericus*) is the highest for absorbing CO_2 based on the NDVI model.

In contrast, the rubber plant or rubber banyan tree (*Ficus elastica*) is the highest for absorbing CO_2 based on the MSARVI and SAVI models. Rudraksha tree and rubber plant or rubber banyan tree have high index values ranging from 0.67 to 0.77. Rudraksha tree (*Elaeocarpus sphaericus*) and rubber plant or rubber banyan tree (*Ficus elastica*) can be used as an alternative to absorb CO_2 emissions. However, further analysis of the morphology and time or length of growth of the two tree species for urban areas is needed.

4. Conclusion

Modeling the estimation of the CO_2 absorption capacity of urban trees using the vegetation index approach and remote sensing data effectively produces models with relatively small error results. Approximately 10,102 trees with 54 types/species have been successfully identified in Kalicacing and Mangunsari Urban Villages. NDVI, SAVI, and MSARVI have error rates ranging from 0.2, indicating that the model is still reasonable to predict. The MSARVI index has the smallest RMSE, which is 0.285, because it better represents the actual content of tree biomass, which is in line with the high level of the greenness of the tree canopy from the image and also because it has reduced the effects of soil background and atmospheric disturbances. The estimated CO_2 absorption capacity of trees in Kalicacing and Mangunsari Villages tends to be moderate to high. The range of the ability of trees in Kalicacing and Mangunsari Villages to absorb CO_2 emissions is 0.32 to 2.26 tons/tree. The trees with the highest CO_2 absorption capacity are the Rudraksha tree (*Elaeocarpus sphaericus*) and the rubber banyan tree or rubber plant (*Ficus elastica*). Both trees can be used as alternatives to absorb CO_2 emissions, and their sustainability must be maintained to contribute generously to absorbing CO_2 emissions. This study is limited to each tree's ability and can only recognize 54 types/species of trees in both villages. Therefore, in further research, remote sensing data can be analyzed temporally to determine the ability of CO_2 absorption of trees each year. Calculating emissions related to motorized vehicles, industry, and households is also necessary. This can determine the stability of trees in urban areas in absorbing CO_2 per year and CO_2 emission inputs.

Acknowledgment

The author is grateful to the Faculty of Geography, Gadjah Mada University, and the Public Works and Spatial Planning Office of Salatiga for providing aerial photography data of Salatiga City as well as the National Unity and Politics Agency of Salatiga City for granting permission for field research activities. The author is also grateful to the RTA Program with NUMBER: 5286/UN1.P1/PT.01.03/2024 for providing the research scheme.

References

[1] World Meteorological Organization, (2024). *State of the Global Climate 2023*. Reading, Switzerland: Publications Board World Meteorological Organization, 2024. [E-book] Available: https://portal.inmet.gov.br/uploads/notastecnicas/1347_Statement_2023_en.pdf.

[2] World Meteorological Organization, (2023). *State of the Global Climate 2022*. Reading, Switzerland: Publications Board World Meteorological Organization, 2023. [E-book] Available: https://wmo.int/publication-series/state-of-global-climate-2022.

[3] Intergovernmental Panel on Climate Change (IPCC), (2022). *Climate Change 2022 Mitigation of Climate Change Summary of Policymakers*. Reading, Switzerland: World Meteorological Organization, 2023. [E-book] Available: https://www.ipcc.ch/report/ar6/wg3/

[4] Khodakarami, L., Pourmanafi, S., Soffianian, A. R. and Lotfi, A. (2022). Modeling Spatial Distribution of Carbon Sequestration, CO_2 Absorption, and O_2 Production in an Urban Area: Integrating Ground-Based Data, Remote Sensing Technique, and GWR Model. *Earth and Space Science*, Vol. 9. https://doi.org/10.1029/2022EA002261.

[5] Angin, R., Setyaningtyas, R. and Adawiyah, P. R., (2022). Using the IPCC Formula to Calculate CO_2 Emissions from Everyday Motorized Vehicles as the Baseline for Climate Change Mitigation Policies. *IOP Conference Series: Earth and Environmental Science, ICST 2024, Yogyakarta, Indonesia, April 23-24, 2022.*

[6] Abbate, S., Di Paolo, L., Carapellucci, R. and Cipollone, R., (2021). Carbon Uptake Dynamics Associated with the Management of Unused Lands for Urban CO_2 Planning. *Renewable Energy*, Vol. 178. https://doi.org/10.1016/j.renene.2021.06.124.

[7] Rachmayanti, L. and Mangkoedihardjo, S., (2020). Evaluasi dan Perencanaan Ruang Terbuka Hijau (RTH) Berbasis Serapan Emisi Karbon Dioksida (CO_2) di Zona Tenggara Kota Surabaya (Studi Literatur dan Kasus) [Evaluation and Planning of Green Open Space (GOS) Based on Carbon Dioxide (CO_2) Emission Absorption in the Southeast Zone of Surabaya City (Literature and Case Studies)]. *Jurnal Teknik ITS*, Vol. 9(2), 107-114. http://dx.doi.org/10.12962/j23373539.v9i2.54854.

[8] Purwanti, S., (2022). Memaksimalkan Fungsi Taman Kota Sebagai Ruang Terbuka Publik [Maximizing the Function of City Parks as Public Open Spaces]. *Jurnal Jendela Inovasi Daerah*, Vol. 5. https://doi.org/10.56354/jendelainovasi.v5i1.114.

[9] Brown, S., (1997). Reading, Urbana: A Forest Resources Assessment Publication. [E-book] Available: https://www.fao.org/4/w4095e/w4095e00.htm.

[10] Rahmatika, I., Hidayati, I. N., Suharyadi, R. and Nurjani, E., (2023). Carbon Stock Estimation from Vegetation Biomass Using Spot-7 Imagery. *Indonesian Journal of Geography*, Vol. 55, 385-396. https://doi.org/10.22146/ijg.78690.

[11] Nurteisa, Y. T., (2016). *Pemanfaatan Teknologi Foto Udara Format Kecil untuk Kajian Perencanaan Jaringan Sanitasi Komunal Kawasan Perkotaan [Utilization of Small Format Aerial Photography Technology for Urban Area Communal Sanitation Network Planning Studies]*, Thesis. Master of Remote Sensing., Universitas Gadjah Mada.

[12] Fadillah, M. A., Bashit, N., Qoyimah, S., Susilo, H. and Apriyanti, D., (2023). Analysis of Vegetation Carbon Stock Estimation Using Remote Sensing with the Light Use Efficiency Method in Penggaron Forest, Ungaran City, Semarang Regency, Central Java Province. *Elipsoida : Jurnal Geodesi dan Geomatika*, Vol. 06(1), 32–42. https://doi.org/10.14710/elipsoida.2023.18829.

[13] Siwi, S. E., (2015). Estimation of Green Vegetation Biomass Content Using Remote Sensing Data. *Prosiding Pertemuan Ilmiah Tahunan XX dan Kongres VI Masyarakat Ahli Penginderaan Jauh Indonesia (MAPIN)*, 744–752.

[14] Jensen, J. R., (2015). *Introductory Digital Image Processing: A Remote Sensing Perspective (4th Edition)*. Columbia: Pearson Education.

[15] Bhatt, A., Ghosh, S. K. and Kumar, A., (2018). Spectral Indices Based Object Oriented Classification for change Detection Using Satellite Data. *International Journal of System Assurance Engineering and Management*, Vol. 9(1), 33–42. https://doi.org/10.1007/s13198-016-0458-7.

[16] Salsabila, H. N., (2021). *Comparison of Vegetation Index Transformation and Forest Canopy Density (FCD) for Canopy Density Mapping in Part of the Mount Arjuno-Welirang Area.* Gadjah Mada University, 2021.

[17] Ash-Shidiq, I. P., Supriatna, S., Darmawan, A., Warta, Z., Molidena, E., Valla, A., Hisan, Firdaus, M. I., Zakaria, N. A., Maufiroh, S., Pradana, M. R. and Putera, D. A., (2024). Biomass Stock Estimation Using Landsat 8 Imagery in Bukit Tigapuluh National Park, Riau. *IOP Conference Series: Earth and Environmental Science, IcoSAG 2022, Depok, Indonesia, November*. Vol. 1291(1). https://doi.org/10.1088/1755-1315/1291/1/012 019.

[18] Somvanshi, S. S. and Kumari, M., (2020). Comparative analysis of Different Vegetation Indices with Respect to Atmospheric Particulate Pollution Using Sentinel Data. *Applied Computing & Geosciences*, Vol. 7. https://doi.org/10.1016/j.acags.2020.100032.

[19] Regional Planning Research and Development Agency, (2023). *Study of Greening Potential in Water Recharge Areas.* Salatiga Indonesia, 2023.

[20] Ming, T., De Richter, R., Liu, W. and Caillol, S., (2014). Fighting Global Warming By Climate Engineering: Is the Earth radiation Management and the Solar Radiation Management any Option for Fighting Climate Change. *Renewable and Sustainable Energy Reviews*, Vol. 31, 792–834. https://doi.org/10.1016/j.rser.2013.12.032.

[21] Halder, B., Bandyopadhyay, J. and Banik, P., (2021). Monitoring the Effect of Urban Development on Urban Heat Island Based on Remote Sensing and Geo-Spatial Approach in Kolkata and Adjacent Areas, India. *Sustainable Cities and Society*, Vol. 74. https://doi.org/10.1016/j.scs.2021.103186.

[22] Huete, (1988). *A Soil-Adjusted Vegetation Index (SAVI). Environmental Science. Remote Sensing of Environment*. 295–309, https://doi.org/10.1016/0034-4257(88)90106-X.

[23] Bannari, A., Ozbakir, A. and Langlois, A., (2007). Spatial Distribution Mapping of Vegetation Cover in Urban Environment using TDVI for Quality of Life Monitoring. *IEEE International Symposium on Geoscience and Remote Sensing*, 679–682. https://doi.org/10.1109/IGARSS.2007.4422887.

[24] Leckie, D. G., Walsworth, N. and Gougeon, F. A., (2016). Identifying Tree Crown Delineation Shapes and Need for Remediation on High Resolution Imagery Using an Evidence Based Approach. *ISPRS Journal of Photogrammetry and Remote Sensing*, Vol. 114, 206-227, https://doi.org/10.1016/j.isprsjprs.2016.02.005.

[25] McCoy, R. M., (2005). *Field Methods in Remote Sensing*. New York, The Guilford Press.

[26] Rana, P., St-Onge, B., Prieur, J. F., Budei, B. C., Tolvanen, A. and Tokola, T., (2022). Effect of Feature Standardization on Reducing the Requirements of Field Samples for Individual Tree Species Classification Using ALS 259 Data. *ISPRS Journal of Photogrammetry and Remote Sensing*, Vol. 184, 189-202. https://doi.org/10.1016/j.isprsjprs.2022.01.003.

[27] Hidayati, I. N., Suharyadi, R. and Danoedoro, P., (2018). Exploring Spectral Index Band and Vegetation Indices for Estimating Vegetation Area. *The Indonesian Journal of Geography*, Vol. 50, 211-221. https://doi.org/10.22146/ijg.38981.

[28] Krisnawati, H., Adinugroho, W.C. and Imanuddin, R., (2012). *Model-Model Alometrik untuk Pendugaan Biomassa Pohon pada Berbagai Tipe Ekosistem Hutan di Indonesia [Allometric Models for Estimating Tree Biomass in Various Types of Forest Ecosystems in Indonesia]*. Reading, Bogor: Badan Penelitian dan Pengembangan Kehutanan Kementerian Kehutanan. [E-book] http://incas.menlhk.go.id/wp-content/uploads/2015/11/Monograf_Model_Model_Alometrik.pdf.

[29] Robinson, D. T., Brown, D. G. and Currie, W. S., (2009). Modelling Carbon Storage in Highly Fragmented and Human-Dominated Landscapes: Linking Land-Cover Patterns and Ecosystem Models. *Ecological Modelling*, Vol. 220(9–10), 1325–1338, https://doi.org/10.1016/j.ecolmodel.2009.02.020.

[30] Food and Agriculture Organization of the United Nations, (2020). *Global and Regional Estimates of Carbon Stocks and Stock Changes 1990–2020*. Rome, Italia.

[31] Yudithia, F. A., Jaelani, L. M. and Handayani, H. H., (2021). Analysis of the Distribution of Biodiversity in Trees and its Potential in Absorbing Carbon Emissions in Urban Areas Using Aerial Photo and Lidar Data (Case Study: Darmo Urban Village, Surabaya City). *Jurnal Teknik ITS*, Vol. 9, 41-47. http://dx.doi.org/10.12962/j23373539.v9i2.53674.

[32] Akbar, T. and Sosilawati, E., (2019). Menghitung Cadangan Karbon yang Tersimpan di Taman Purbakala Bukit Siguntang Palembang Sumatera Selatan [Calculating Carbon Reserves Stored in the Bukit Siguntang Archaeological Park, Palembang, South Sumatra]. *Sylva: Jurnal Penelitian Ilmu-Ilmu Kehutanan*, Vol. 8(1), 21-29. https://doi.org/10.32502/sylva.v8i1.1856.

[33] Sumida, A., Miyaura, T. and Torii, H., (2013). Relationships of Tree Height and Diameter at Breast Height Revisited: Analyses of Stem Growth Using 20-Year Data of An Even-Aged Chamaecyparis Obtusa Stand. *Tree physiology*, Vol. 33, 106-118. https://doi.org/10.1093/treephys/tps127.

[34] Meyer, V., Saatchi, S., Clark, D. B., Keller, M., Vincent, G., Ferraz, A., Espírito-Santo, F., d'Oliveira, M. V. N., Kaki, D. and Chave, J., (2018). Canopy Area of Large Trees Explains Aboveground Biomass Variations Across Neotropical Forest Landscapes. *Biogeosciences*, Vol. 15, 3377-3390. https://doi.org/10.5194/bg-15-3377-2018.

[35] Suryandari, P., Astiani, D. and Dewantara, I., (2019). Pendugaan Karbon Tersimpan Pada Tegakan Di Kawasan Arboretum Sylva Universitas Tanjungpura [Estimation of Stored Carbon in Stands within the Sylva Arboretum Area, Tanjungpura University. *Jurnal Hutan Lestari*, Vol. 7(1). 114–122, https://doi.org/10.26418/jhl.v7i1.31171.

[36] Astuti, C. C., (2017). Analisis Korelasi Untuk Mengetahui Keeratan Hubungan Antara Keaktifan Mahasiswa Dengan Hasil Belajar Akhir [Correlation Analysis to Determine the Strength of the Relationship Between Student Activeness and Final Learning Outcomes]. *JICTE (Journal of Information and Computer Technology Education)*, Vol. 1(1), 1-7. https://doi.org/10.21070/jicte.v1i1.1127.

[37] De Carvalho, O. A., Guimarães, R. F., Silva, N. C., Gillespie, A. R., Gomes, R. A. T., Silva, C. R. and De Carvalho, A. P. F., (2013). Radiometric Normalization of Temporal Images Combining Automatic Detection of Pseudo-Invariant Features from the Distance and Similarity Spectral Measures, Density Scatterplot Analysis, and Robust Regression. *Remote Sensing*, Vol. 5, 2763-2794. https://doi.org/10.3390/rs5062763.

[38] Yudistira, R., Meha, A. I. and Prasetyo, S. Y. J., (2019). Perubahan Konversi Lahan Menggunakan NDVI, EVI, SAVI dan PCA pada Citra Landsat 8 (Studi Kasus: Kota Salatiga) [Land Conversion Changes Using NDVI, EVI, SAVI and PCA on Landsat 8 Imagery (Case Study: Salatiga City)]. *Indonesian Journal of Computing and Modeling*, Vol. 2(1), 25-30. https://ejournal.uksw.edu/icm/article/view/2537.

[39] Oke, E. O., Adeyi, O., Okolo, B. I., Adeyi, J. A., Ayanyemi, J., Osoh, K. A. and Adegoke, T. S., (2020). Phenolic Compound Extraction from Nigerian Azadirachta Indica Leaves: Response Surface and Neuro-Fuzzy Modelling Performance Evaluation with Cuckoo Search Multi-Objective Optimization. *Results in Engineering*, Vol. 8. https://doi.org/10.1016/j.rineng.2020.100160.

[40] Zeng, L., Wardlow, B. D., Xiang, D., Hu, S. and Li, D., (2020). A Review of Vegetation Phenological Metrics Extraction Using Time-Series, Multispectral Satellite Data. *Remote Sensing of Environment*, Vol. 237. https://doi.org/10.1016/j.rse.2019.111511.

[41] Lu, D., Chen, Q., Wang, G., Liu, L., Li, G. and Moran, E., (2016). A Survey of Remote Sensing-Based Aboveground Biomass Estimation Methods in Forest Ecosystems. *International Journal of Digital Earth*, Vol. 9(1), 63-105. https://doi.org/10.1080/17538947.2014.990526.